HHS Public Access

Author manuscript

Stem Cells. Author manuscript; available in PMC 2017 April 01.

Published in final edited form as:

Stem Cells. 2016 April ; 34(4): 1068–1082. doi:10.1002/stem.2293.

Loss of Folliculin disrupts hematopoietic stem cell quiescence and homeostasis resulting in bone marrow failure

Masaya Baba[1,5,7], **Hirofumi Toyama**[2,7], **Lei Sun**[4,7], **Keiyo Takubo**[3], **Hyung-Chan Suh**[4], **Hisashi Hasumi**[1], **Ayako Nakamura-Ishizu**[2], **Yukiko Hasumi**[1], **Kimberly D. Klarmann**[4], **Naomi Nakagata**[6], **Laura S. Schmidt**[1,4], **W. Marston Linehan**[1,8], **Toshio Suda**[2,5,8], and **Jonathan R. Keller**[4,8]

[1]Urologic Oncology Branch, Center for Cancer Research, National Cancer Institute, National Institutes of Health, Bethesda, MD 20892, USA

[2]Department of Cell Differentiation, The Sakaguchi Laboratory of Developmental Biology, School of Medicine, Keio University, 35 Shinano-machi, Shinjuku-ku, Tokyo 160-8582, Japan

[3]Department of Stem Cell Biology, Research Institute, National Center for Global Health and Medicine, Tokyo 162-8655, Japan

[4]Mouse Cancer Genetics Program and [4]Basic Science Program, Leidos Biomedical Research, Inc., Center for Cancer Research, Frederick National Laboratory for Cancer Research, Frederick, MD 21702, USA

[5]International Research Center for Medical Sciences (IRCMS), Kumamoto University, Kumamoto, 〒 860-0811, Japan

[6]Division of Reproductive Engineering, Center for Animal Resources and Development (CARD), Kumamoto University, Kumamoto, 〒 860-0811, Japan

Abstract

Folliculin (FLCN) is an autosomal dominant tumor suppressor gene that modulates diverse signaling pathways required for growth, proliferation, metabolism, survival, motility and adhesion. FLCN is an essential protein required for murine embryonic development, embryonic stem cell (ESC) commitment, and *Drosophila* germline stem cell maintenance, suggesting that Flcn may be required for adult stem cell homeostasis. Conditional inactivation of *Flcn* in adult hematopoietic stem/progenitor cells (HSPCs) drives HSC into proliferative exhaustion resulting in the rapid depletion of HSPC, loss of all hematopoietic cell lineages, acute bone marrow failure, and mortality after 40 days. HSC that lack *Flcn* fail to reconstitute the hematopoietic compartment in recipient mice, demonstrating a cell-autonomous requirement for *Flcn* in HSC maintenance. Bone

[8]Correspondence should be addressed to, Jonathan R. Keller, kellerjo@mail.nih.gov, Phone: 301-846-1461; Fax: 301-846-6646, Toshio Suda., sudato@z3.keio.jp, Phone: -81-3-5363-3473; Fax: +81-3-5363-3474, W. Marston Linehan, linehanm@mail.nih.gov, Phone: 301-496-6353; Fax: 301-402-0922.

[7]Contribute to this study as a first author

Authorship Contribution: M.B.; H.T.;L.S.; L.S.S; J.R.K; designed and performed research, analyzed data, and wrote the manuscript; K.T.;H-C.S.; K.D.K.; designed and performed research, and analyzed data; H.H. ; A.N-I.; Y.H., N.N.; performed research; W.M.L. Final approval of manuscript, wrote manuscript, financial support; T.S.; designed research, analyzed data, and wrote manuscript.

Conflict of Interest Disclosure: The authors declare no competing financial interests.

marrow cells (BMC) showed increased phosphorylation of Akt and mTorc1, and extramedullary hematopoiesis was significantly reduced by treating mice with rapamycin *in vivo*, suggesting that the mTorc1 pathway was activated by loss of *Flcn* expression in hematopoietic cells *in vivo*. Tfe3 was activated and preferentially localized to the nucleus of *Flcn* knockout (KO) HSPCs. Tfe3 overexpression in HSPCs impaired long term hematopoietic reconstitution *in vivo*, recapitulating the *Flcn* KO phenotype, and supporting the notion that abnormal activation of Tfe3 contributes to the *Flcn* KO phenotype. *Flcn* KO mice develop an acute histiocytic hyperplasia in multiple organs, suggesting a novel function for *Flcn* in macrophage development. Thus, Flcn is intrinsically required to maintain adult HSC quiescence and homeostasis, and *Flcn* loss leads to bone marrow failure and mortality in mice.

Keywords

Hematopoiesis; Stem Cells; Bone Marrow Failure; FLCN

Introduction

Birt-Hogg-Dubé (BHD) syndrome is caused by germline mutations in the *folliculin* (*FLCN*) gene, and is characterized by benign hair follicle hamartomas (fibrofolliculoma), lung cysts, spontaneous pneumothorax, and increased risk of kidney cancer (1–3). Homozygous deletion of *Flcn* in mice results in embryonic lethality, and conditional inactivation of *Flcn* in adult mouse kidney epithelial cells leads to uncontrolled cell proliferation resulting in polycystic kidneys and renal failure by three weeks of age (4–6). *Flcn* heterozygous mice survive and appear normal; however, these mice progress to kidney neoplasia subsequent to loss of heterozygosity at the *Flcn* locus, suggesting that *Flcn* functions as a tumor suppressor gene (4, 7, 8).

Accumulating evidence suggest that Flcn is a multifunctional protein that modulates a number of cell signaling pathways important in cell metabolism, growth, proliferation, adhesion, and survival (9, 10). For example, FLCN and FLCN-interacting partners FNIP1/2 are found in complex with AMPK, a key molecule in cellular energy and nutrient sensing, which negatively regulates mTORC1, suggesting that FLCN/FNIP might affect AMPK-mTORC1 signaling (11–13). Targeted deletion of *Flcn* in mouse lung epithelial cells results in decreased E-cadherin and Lkb1 expression, which negatively affects Ampk function and impairs lung epithelial cell survival and function (14). Loss of *Flcn* function in murine cardiomyocytes leads to elevated *Ppargc1a* expression that drives increased mitochondrial biogenesis and ATP production, which can also lead to the activation of mTorc1(15). Loss of *Flcn* in some human and mouse kidney tumors leads to the activation of Raf-Mek-Erk and Akt-mTor pathways, suggesting that loss of *Flcn* may contribute to kidney neoplasia via activation of these pathways (4, 5). However, other studies indicate that mTorc1 is not activated by loss of *Flcn*, indicating that activation of mTorc1 may be cell type and context dependent (7, 16, 17). Loss of *Flcn* reduces the expression of genes involved in TGF-β signaling in ESC and kidney cancer cell lines, and contributes to tumor growth (18, 19). While Flcn has a central role in transducing cell signals that regulate many cell processes,

the precise molecular targets of Flcn and downstream signaling pathways regulated by Flcn remain active areas of research.

While loss of *Flcn* function *in vivo* contributes to the development of kidney cancer in mice, the nature of the cell populations that contribute to kidney cancer have not been characterized. In this regard, many tissues and organs are maintained throughout life by stem and progenitor cell populations, and these cell populations are frequently the cellular source of the malignancies that arise in these tissues with age (20). Since the cellular pathways affected by Flcn are required for the function of many cell types, we hypothesized that Flcn may be required for adult stem and progenitor cell homeostasis (21–25).

Hematopoietic stem cells (HSC) sustain multi lineage blood cell development over the life of the animal by their unique ability to proliferate and self-renew and/or differentiate (26, 27). HSCs are protected from proliferative exhaustion by remaining in a quiescent or dormant state, and are regulated, in part, by intrinsic cell signaling programs. For example, loss of *Pten*, *Tsc1/2*, and *Lkb1* leads to hyperactivation of the mTorc1 pathway, increased HSC proliferation, exhaustion and loss of HSC function, and in some cases leukemogenesis (21, 23, 24, 28, 29). Since Flcn has a role in regulating the Lkb1-Ampk-mTorc1 signaling axis, we considered if Flcn might be required for HSC cell quiescence, cell division, tissue maintenance and regeneration (14). Therefore, we conditionally inactivated *Flcn* in adult murine hematopoietic cells, and report here for the first time that loss of *Flcn* in hematopoietic cells drives HSPCs into proliferative exhaustion resulting in the rapid depletion of HSPC and all hematopoietic cell lineages, and acute bone marrow failure.

Materials and Methods

Animals

The mice carrying *Flcn* floxed alleles *(Flcn^{f})* were generated as previously described(5). To conditionally delete the *Flcn^{f}* allele, a *Mx1-Cre* transgene was introduced into *Flcn$^{f/f}$* mice, and at 6 weeks of age *Flcn$^{f/f}$;Mx1-Cre+* mice, *Flcn$^{f/f}$*, and *Flcn$^{f/+}$;Mx1-Cre+* mice were injected with 300μg of polyinosinic–polycytidylic acid solution (pIpC) dissolved in physiological water (NaCl 0.9%) (tlrl-pic, Invivogen or P1530, Sigma-Aldrich) 2 or 3 times every other day. The day of last injection was defined as day 0. PCR genotyping was performed as previously described. All animal experiments were approved by the National Cancer Institute or Keio University and performed in accordance with the guidelines of Keio University for animal and recombinant DNA, or NCI Animal Care and Use Committee.

Antibodies

The following monoclonal antibodies (Abs) were used for flow cytometry and cell sorting: anti-c-Kit Microbeads (Miltenyi Biotec), anti-c-Kit (2B8, BD Biosciences / Biolegend), anti-Sca-1 (E13–161.7, BD Biosciences / Biolegend), anti-CD45.1 (A20, Biolegend), anti-CD45.2 (104, BD Biosciences), anti-CD4 (RM4–5, BD Biosciences), anti-B220 (RA3–6B2, BD Biosciences), anti-TER-119 (TER-119, Biolegend), anti-Gr-1 (RB6–8C5, BD Biosciences/Biolegend), anti-Mac-1 (M1/70, BD Biosciences), anti-CD71 (C2, BD Biosciences), anti-CD43 (S7, BD Biosciences), anti-CD16/32 (2.4G2, BD Biosciences),

anti-Ki67 (B56, BD Biosciences), anti-CD34 (RAM34, eBioscience), anti-CD135 (A2F10, Biolegend), The primary Ab used for immunocytochemistry (ICC) was goat anti-Tfe3 (p-16; Santa Cruz Biotechnology). Anti-phospho mTor (Ser2448), anti-phospho Akt (Thr308), and anti-beta actin from Cell Signaling were used for western blotting.

Flow cytometry

Mice were euthanized by CO2 asphyxiation for analyses. Dissected femurs and/or tibiae were flushed in 1% BSA/PBS. Spleens were cut into small pieces and mashed on a 40μm cell strainer (BD Biosciences). Cells were stained with the indicated antibodies, and analyzed by FACS-LSRII or FACS-Canto. Mouse HSPCs were purified from the mononuclear cells (MNCs), obtained by hemolysis with NH_4Cl, followed by lineage depletion with lineage-specific antibodies (a mixture of CD4, CD8, B220, TER-119, Mac-1, and Gr-1), and flow cytometry cell sorting with antibodies directed against interleukin (IL)–7 receptor, c-Kit, Sca-1, CD34, CD135 and anti- CD16/32 by the use of FACSAria III (BD Biosciences) as previously described (30). For Ki67 staining, BMCs were fixed and permeabilized with Cytofix/Cytoperm Buffer (BD Pharmigen) at R.T. for 15 minutes following surface marker staining, then incubated in Cytoperm Plus Buffer (BD Pharmigen) for 10 min. at 4°C. The cells were stained with Ki67 antibody (BD Pharmigen) in Perm/Wash Buffer (BD Pharmigen) at R.T. 30 min., and then cells were incubated in Perm/Wash Buffer with FxCycle Stain at 4°C overnight.

Quantitative RT-PCR (qPCR)

Total RNA was isolated using TRIzol Reagent (Invitrogen), and reverse transcribed to cDNA using SuperScript III reverse transcriptase Kit (Invitrogen). qPCR assays were performed with the ABI 7300 Real-Time PCR System (Applied Biosystems) and the SYBR Green PCR Master Mix (Fermentas). The primer sequences for *Flcn* are as follows: forward 5'-gctcctgaaggcatgcggtagca-3' , reverse 5'-cagcaagcttctccatctggaccag-3'. Primers for *Tfe3* are purchased from TaKaRa Bio. Signal intensity obtained from real-time PCR System was described in relative units; each value was normalized to β-actin with the following sequences: forward 5'- gacatggagaagatctggca −3', reverse 5'- ggtctcaaacatgatctgggt −3'.

Western blot analysis

Cell pellets were flash frozen in liquid nitrogen immediately. Frozen cell pellets were lysed on ice in RIPA buffer (20 mM Tris-HCl, pH 7.5, 150 mM NaCl, 1 mM EDTA, 1.0% Triton X-100, 0.5% deoxycholate, 0.1% sodium dodecylsufate, PhosSTOP Phosphatase Inhibitor Cocktail (Roche), and Complete Protease Inhibitor Cocktail (Roche), followed by centrifugation at 13,200g for 30 minutes. Protein concentrations of cleared supernatants were measured with BCA Protein Assay Kit (Pierce). SDS-sample buffer was added and samples were boiled for 5 minutes.

Virus Transduction

Murine *Tfe3* cDNA was subcloned upstream of IRES-EGFP in pMY-IRES-EGFP. After transfection of plasmid DNA into Plat-E cells by FuGENE (Roche) using CombiMag (Funakoshi), supernatants were used to transduce LSK cells cultured on a U-bottomed

fibronectin-coated plate in SF-O3 medium (Sanko Junyaku) with 100 ng/ml SCF and 100 ng/ml thrombopoietin (TPO) for 16 hr. After 48 hours, GFP+ cells (LSK Tfe3 and control LSK GFP, respectively) were sorted by FACS and used for ICC, qPCR and BMT.

Bone marrow transplantation

BMC were prepared from CD45.2+ *Flcn*$^{fl/+}$;Mx1-Cre+, *Flcn*$^{fl/fl}$;Mx1-Cre- and *Flcn*$^{fl/fl}$;Mx1-Cre+ mice, respectively without hemolysis. BMCs were transplanted (~1×10^6 cells / recipient) intravenously into lethally irradiated CD45.1+ recipient mice, together with CD45.1+ competitor cells without hemolysis (~1×10^6 cells / recipient). Six weeks after BMT, peripheral blood cells (PBC) were analyzed for chimerism using flow cytometry. One week later, the recipient mice were treated with 300μg pIpC per mouse 3 times every 2 days. In Figure 7, BMCs were obtained from CD45.2+ mice and the LSK fraction was sorted from these BMCs. LSK cells were transduced with retroviral vectors that co-express *Tfe3* and GFP or control retroviral vectors, and then were transplanted (~33000 cells/recipient) intravenously into lethally irradiated CD45.1+ mice. PB chimerism was analyzed monthly after BMT.

Immunocytochemistry (ICC)

LT-HSCs, LSK Tfe3 and LSK GFP were sorted, respectively, and centrifuged by Cytospin 4 (Thermo Scientific) on a glass slide (FRC-04, Matsunami). Slides were washed with PBS and incubated with Protein Block Serum-Free Ready-to-use (PBSFR) blocking solution (Dako) to inhibit non-specific staining, followed by incubation with PBSFR-diluted primary Ab overnight at 4°C. After washing with PBS, slides were stained with PBSFR-diluted corresponding secondary Ab for 90 minutes at room temperature. Fluorescent images were obtained using a confocal laser scanning microscope (FV1000, Olympus).

Results

Flcn is required for the development of myeloid, erythroid and lymphoid lineages

Flcn is expressed in HSPCs, and in many other tissues (Fig 1S). Homozygous *Flcn* deletion in mice results in early embryonic lethality, suggesting its fundamental role in development(4). To determine if Flcn is required for hematopoiesis we crossed conditional *Flcn* knockout mice (*Flcn*$^{f/f}$) with *Mx1-Cre*$^{+}$ transgenic mice. *Flcn* was efficiently deleted in BMC and spleen cells in *Flcn*$^{f/f}$*;Mx1-Cre*$^{+}$ (*Flcn* KO) mice 5 and 21 days after pIpC injection (Fig 1A) (31) resulting in loss of *Flcn* mRNA (Fig 1B) and protein expression (Fig 1C) compared to *Flcn* WT (*Flcn*$^{f/f}$*;Mx1-Cre*$^{-}$) mice. Strikingly, all *Flcn* KO mice were moribund by 40 days after pIpC injection (median survival 27 days, $p<0.0001$) (Fig 1D) and had developed acute splenomegaly, which was significant beginning one week after the last pIpC injection, whereas *Flcn* WT mice were unaffected (Fig 1E–F). Additionally, femurs from *Flcn* KO mice at day 21 were pale compared to *Flcn* WT mice, suggesting a potential defect in erythroid development (Fig 1G). H&E staining at day 21 revealed that the BM was hypoplastic (Fig 1H), and total BM cellularity was dramatically reduced more than 90% relative to *Flcn* WT mice, suggesting that Flcn is required for hematopoiesis (Fig 1I). To determine the effect of Flcn loss on hematopoiesis, we analyzed lineage development by flow cytometry in BM and spleen at day 21. Erythroid differentiation was arrested in BM at

an early developmental stage with the accumulation of $CD71^{+}Ter119^{-/lo}$ cells, and loss of $CD71^{+}Ter119^{+}$ erythroblasts and $CD71^{-}$ $Ter119^{+}$ maturing red cells (Fig. 2A). Concomitantly, we observed a significant increase in extramedullary hematopoiesis in *Flcn* KO spleen (Fig 1E), with significant increases in immature $CD71^{+}Ter119^{-/lo}$ and $CD71^{+}Ter119^{+}$ erythroid cells (Fig 2A). A complete blood count (CBC) analysis of *Flcn* KO confirmed that these mice were severely anemic (RBC and Hb levels), and showed a profound thrombocytopenia (Table S1). Thus, Flcn is required for normal erythroid development.

We also uncovered a severe developmental block in myelopoiesis resulting in the absence of mature neutrophil production in BM. $Gr1^{Hi}Mac\text{-}1^{Hi}$ neutrophils were reduced by >95% in *Flcn* KO BM, while $Gr\text{-}1^{lo}Mac\text{-}1^{Hi}$ cells were significantly increased (Fig. 2B). Expansion of $Gr1^{lo}Mac\text{-}1^{Hi}$ cells was also observed in *Flcn* KO spleens (Fig. 2B), and as expected, few $Gr\text{-}1^{lo}Mac\text{-}1^{Hi}$ cells and $Gr1^{Hi}Mac\text{-}1^{Hi}$ neutrophils were present in *Flcn* WT spleen cells. While BMC showed a significant reduction in neutrophils in *Flcn* KO mice, the CBC analysis of *Flcn* KO PB showed no difference in neutrophil counts (NE). We analyzed the morphology of cells present in PB smears of *Flcn* KO mice, and determined that mature neutrophils were present in PB of Flcn WT mice, while mature and immature neutrophils were present in the PB of Flcn KO mice, which could account for the absence of neutropenia in the CBC analysis (Figure S4). Thus, neutrophil development is blocked in bone marrow of *Flcn* KO mice with concomitant expansion of $Gr\text{-}1^{lo}Mac\text{-}1^{Hi}$ cells, which also expressed higher levels of Mac-1.

B cell development was arrested at the B cell progenitor (pre-pro- and pro-B cell) stage in *Flcn* KO BM, which resulted in the loss of immature $CD43^{-}B220^{lo}$ and mature $CD43^{-}B220^{hi}$ B cells (Fig 2C); however, using BM cellularity to normalize the data, we found that B cells at all stages of development were significantly reduced. Total thymocyte cellularity was significantly decreased in *Flcn* KO mice (Fig. 2D, lower left pane1). In addition, the total number of rapidly dividing maturing CD4+CD8+ cells were significantly reduced (>75%), when we combined percentage of CD4+CD8+ cells (Fig. 2, upper right panel) and total thymocyte cellularity (Fig. 2, lower right panel). In comparison, the more mature single positive cells (CD4+ and CD8+ cells) showed a trend toward reduction, but were not statistically different at the time of this analysis (Fig. 2D, lower right panel). Thus, these data support a requirement for Flcn in erythroid, myeloid and lymphoid cell development in BM.

Loss of *Flcn* leads to HSPC exhaustion and bone marrow failure

The complete absence of mature blood cell development in *Flcn* KO BM suggested a requirement for Flcn in HSPC development; therefore, we evaluated the HSPC compartment by flow cytometry. The absolute number of $Lin^{-}Sca1^{+}c\text{-}Kit^{+}$ (LSK) cells including HSC and all multipotential stem/progenitor cell populations was dramatically reduced in *Flcn* KO BM seven days after pIpC administration reflecting the severity of the BM hypocellularity (Fig 3A). Also, the numbers of long term (LT)-HSCs, short term (ST)-HSCs and multipotential progenitors (MPP)s were severely reduced in *Flcn* KO compared to *Flcn* WT BM (*Flcn* WT vs *Flcn* KO LT-HSC: 1,670 vs. 408/mouse, $p \leq 0.05$; ST-HSC: 20,674 vs. 1,373/mouse,

p≤0.01; MPP: 12,327 vs. 456/mouse, p≤0.01) (Fig 3A). Thus, Flcn is required to maintain normal numbers of immunophenotypically-defined LT-HSC, ST-HSC and MPP in BM.

In comparison, HSPCs in *Flcn* KO spleens increased significantly beginning 2 weeks after pIpC injection, and showed significant expansion by 3 weeks (Fig 3B). The absolute number of immunophenotypically-defined LT-HSC, ST-HSC and MPP in *Flcn* KO spleens was increased early after the onset of extramedullary hematopoiesis (Fig 3B). Thus, increased extramedullary hematopoiesis in spleen is concomitant with BM failure in *Flcn* KO mice.

Immunophenotypic analysis of the more committed $Lin^{-}Sca1^{-}c\text{-}Kit^{+}$ (LK) progenitor cells showed that these cells were reduced by more than 80% in *Flcn* KO BM seven days after pIpC administration (Fig 3C). For example, megakaryocyte/erythroid progenitor (MEP) and common myeloid progenitor (CMP) numbers were reduced by greater than 90% in *Flcn* KO BM consistent with the severe anemic phenotype. In comparison, the absolute number of granulocyte/macrophage progenitor (GMP) cells was less affected by *Flcn* loss, although the total numbers were reduced by 60% in *Flcn* KO BM (Fig 3C). In contrast to BM, LK, CMP, GMP and MEP populations were significantly expanded in KO spleen (Fig 3D). Thus, *Flcn* is required to maintain normal numbers of immunophenotypically-defined CMP, MEP and GMP BM progenitor cell populations, and *Flcn* loss results in significant expansion of these progenitors as a consequence of extramedullary hematopoiesis in KO spleen.

Flcn functions as a cell-autonomous regulator of HSPC development

Since *Flcn* can be deleted in HSPC and Niche cells in $Flcn^{f/f}$;*Mx1-Cre*+ mice treated with pIpC, we performed competitive and noncompetitive BM transplantation (BMT) assays to determine if BM failure in *Flcn* KO mice was intrinsic to hematopoietic cells or not. Reconstitution of *Flcn* KO derived CD45.2+ BMC was dramatically decreased after pIpC administration relative to *Flcn* WT CD45.1+ BMCs in competitively transplanted mice over a seven months period (Fig. 4A), demonstrating that defective long-term reconstitution (LTR) activity of *Flcn* KO HSPCs is cell-autonomous (Fig. 4B). In addition, *Flcn* KO and *Flcn* WT BMC were transplanted into lethally irradiated *Flcn* WT recipient mice in the absence of competitive BMC, and pIpC was administered 6 weeks after BMT (Fig.4C). Three weeks after pIpC administration, femurs from mice transplanted with *Flcn* KO BMC were pale (Fig. 4D), and donor BM cellularity was reduced greater than 90% indicating bone marrow failure (Fig. 4E). Lineage analysis of BMCs showed severe maturational blocks in the development and production of erythroid (Fig 4F), myeloid (Fig 4G), and B-cells (Fig 4H), which recapitulates the lineage differentiation defects observed in the $Flcn^{f/f}$;*Mx1-Cre*+ mice, and confirms that *Flcn* is intrinsically required for hematopoietic development. Furthermore, mice transplanted with *Flcn* KO BMCs showed extramedullary hematopoiesis including significant increase in spleen size (Fig. 4I), spleen weight (Fig. 4J), and spleen cellularity (Fig. 4K) at 3 weeks post pIpC administration. FACS analysis of spleen cells showed a total increase in the number of $Gr\text{-}1^{Hi}Mac\text{-}1^{Hi}$ neutrophils and a concomitant increase in the total number of $Gr\text{-}1^{lo}Mac\text{-}1^{Hi}$ cells (Fig. 4L). Furthermore, we observed an expansion of LSK cells in the spleen, which included increased numbers of LT-HSC, ST-HSC and MPPs (Fig. 4M). Finally, the majority (80%) of the lethally irradiated mice transplanted with BMC from *Flcn* KO mice and treated with pIpC after 6 weeks were

moribund after 80 days, while few or no mice transplanted with the BMC from *Flcn* WT mice became moribund (Fig S2). Thus, Flcn is intrinsically required for BMC development, and loss of function leads to BM failure and death.

Flcn is required for HSPC quiescence and survival

To ascertain if loss of the HSPC compartment in the BM was due to increased cell cycling and exhaustion, or apoptosis, we analyzed LSK cells in BM by flow cytometry. *Flcn* KO LSK cells showed significantly fewer cells in G0 relative to *Flcn* WT LSKs (WT vs KO : 26% vs 14%), and a significant increase in S/G2 Ki67-positive cells (WT vs KO : 12% vs. 24%) supporting increased numbers of cycling HSPCs in *Flcn* KO mice (Fig 5A). To confirm that *Flcn* loss causes increased HSPC cycling, we injected a sublethal dose of 5-FU weekly, which is toxic to cycling HSPCs, after pIpC injection. *Flcn* KO mice were moribund by day 15 (median survival 9.5 days, $p<0.0001$), while no effect on *Flcn* WT were observed after three 5-FU injections (Fig 5B). To determine if Flcn affected HSPC survival we analyzed apoptosis in BM by flow cytometry. Annexin V positive apoptotic cells were significantly increased in *Flcn* KO BM compared to *Flcn* WT BM (Fig 5C). Thus, loss of *Flcn* leads to increased HSPC cycling and increased apoptosis, which could contribute to HSC exhaustion, loss of all lineage development, and BM failure.

Loss of *Flcn* function promotes histiocytosis and hemophagocytosis

Flcn KO mice showed severe splenomegaly, which included the expansion of a brightly stained Mac-1+ cell population that expressed low levels of Gr-1 cells in *Flcn* KO spleen (Fig 2B). Histological analysis of the spleen, and other organs including liver, lung, and skin showed an infiltration of histiocytes/macrophages (Fig. 6A–D). Further immunophenotype analysis of the expanding Gr-1^{lo} Mac-1^{Hi} cells in *Flcn* KO BM showed that many cells expressed c-Kit and CD4 (Fig 6G, H). The CD4+ cells did not co-express CD3+ or CD8+ indicating they were not T cells (data not shown). Giemsa stained cytocentrifuge preparations of BMC and spleen cells revealed numerous histiocytes including some that were engulfing erythrocytes, neutrophils and lymphocytes to varying degrees (hemophagocytosis), indicating abnormal macrophage activation (Fig 6E, 6F, Fig 3S). Histiocytes were also observed in PB smears of *Flcn* KO, but not Flcn WT mice (Fig. 4S). Histiocytosis was also observed in splenocytes obtained from chimeric mice transplanted with *Flcn* KO BMC (data not shown), demonstrating that this phenotype was intrinsic to hematopoietic cells. Thus, concomitant with bone marrow failure in *Flcn* KO mice, we observed an expansion of histiocytic cells that expressed high levels of Mac-1 with increased mean fluorescence intensity. Additional studies will be required to reveal the nature of this novel cell population that expands in *Flcn* KO spleen during BM failure, and a more detailed analysis of normal macrophage development.

Hepatosplenomegaly mediated by mTorc1 activation is reversed by treatment with rapamycin

Loss of *Flcn* expression in kidney epithelial cells leads to hyperproliferation, enlarged polycystic kidneys, and kidney cancer, which is correlated with increased Akt and mTorc1 activation (4, 5). To determine if mTorc1 and Akt were activated in *Flcn* KO BMC, we evaluated activation of Akt and mTorc1 phosphorylation by western blot analysis. We

observed increased phosphorylation of threonine 308 on Akt, and serine 2448 on mTor in BMC obtained from mice 5 and 21 days after *Flcn* deletion, suggesting that these pathways were activated (Fig 6I). To determine the physiological significance of mTorc1 pathway activation in *Flcn* KO mice, we treated pIpC treated *Flcn* WT and KO mice with rapamycin for 24 days. Rapamycin treatment markedly reduced the size of *Flcn* KO spleen and liver (Figure 6J, 6K and 6L). In addition, rapamycin reduced the number of HPC in *Flcn* KO BM and spleen (Fig 6M), suggesting that mTorc1 activation promotes increased HPC proliferation in *Flcn* KO mice, and contributes to the extramedullary hematopoiesis by the *Flcn* KO HSPC in the spleen.

Aberrant activation of Tfe3 causes defective HSC activity of *Flcn* KO HSPC

Loss of *Flcn* expression leads to increased translocation of the basic-helix-loop-helix leucine zipper (bHLH)-Zip transcription factor *Tfe3* to the nucleus of mouse embryonic fibroblasts, HeLa and kidney cancer cell lines (32, 33). Loss of *Flcn* in mouse ES cells leads to the nuclear localization of Tfe3, and prevents ES cell differentiation(34). Based on these findings, we hypothesized that Tfe3 nuclear translocation might occur in hematopoietic cells after *Flcn* inactivation. Therefore, we examined Tfe3 localization in cytocentrifuge preparations of *Flcn* KO and *Flcn* WT HSC by immunocytochemistry (ICC) (Fig 7A). Tfe3 was located in the nucleus in 32% of LT-HSCs from *Flcn* WT mice and 67% of LT-HSCs from *Flcn* KO mice (Fig 7A), suggesting that *Flcn* inactivation leads to Tfe3 nuclear translocation, which could contribute to the *Flcn* KO hematopoietic phenotypes. To investigate if Tfe3 might mediate some of the hematopoietic phenotypes in the *Flcn* KO mice, we overexpressed *Tfe3* in HSPC using retroviral vectors, and transplanted these cells in competitive repopulation BMT assays (Fig 7B). LSK cells were transduced with retroviral vectors that expressed GFP and *Tfe3*, or GFP alone, and then GFP+ LSK cells were sorted and stained for Tfe3 to confirm its overexpression and nuclear localization (Fig 7C). *Tfe3* overexpression in transduced LSK cells was confirmed by real-time PCR (Fig 7D). Further, the percentage of donor-derived GFP+ cells was reduced to 10% in mice transplanted with Tfe3-overexpressing LSK cells one month after BMT compared to 28% in control LSK-transplanted mice (Fig. 7E). Tfe3 overexpressing LSK cells continued to show significantly reduced donor reconstitution 2, 3 and 4 months after BMT compared to control LSK cells. The percentages of B cells (B220+) and neutrophils (Gr-1^{Hi}Mac-1^{Hi}) cells were not significantly different, while the percentages of CD8+ and CD4+ cells were reduced in donor PBC of mice transplanted with LSK Tfe3 cells compared to mice transplanted with LSK GFP cells. Thus, development of all lineages was reduced (T cells most affected) (Fig. 7F). In addition, we found that the percentages of Gr-1^{lo}Mac-1^{Hi} cells were increased in the PB of mice transplanted with LSK Tfe3 cells, which is similar to that observed in mice that lack *Flcn* (Fig. 7F). However, we observed no significant differences in spleen weight in mice transplanted with Tfe3-expressing LSK cells (Fig. 7G). It is possible that mTorc1 activation is critical for splenomegaly, since rapamycin treatment significantly affects spleen size in the Flcn KO model (Fig. 6J). Taken together, these results indicate that loss of *Flcn* results in nuclear translocation and activation of Tfe3, which may contribute, in part, to impaired HSPC function in *Flcn* KO mice.

Discussion

The results of gene inactivation studies in mouse kidney, lung and ES cells suggest that *Flcn* may regulate stem cell proliferation and differentiation, and may be required to maintain adult stem cell populations in these and other organs. In this regard, the *Drosophila* ortholog of *FLCN* is required for male germline stem cell maintenance (35). Therefore, we conditionally inactivated *Flcn* in adult BMCs, and discovered a critical role for Flcn in maintaining adult hematopoietic stem cell quiescence and homeostasis. Loss of *Flcn* expression in adult BMC leads to acute BM failure, and mice do not survive due to the severe loss of HSPC, and all hematopoietic lineages. HSC that lack *Flcn* undergo proliferative exhaustion and apoptosis. BM failure was accompanied by extensive extramedullary hematopoiesis and a profound histiocytosis, and these cells were observed to infiltrate many organs, including BM where histiocytic phagocytosis was observed. The phenotypes were broad and dramatic, indicating an essential role of Flcn in maintaining normal hematopoiesis.

HSCs and stem cells in other organs are maintained by a balance between quiescent and cycling states to prevent their exhaustion. We found that Flcn functions to maintain the quiescence of adult HSC. In other studies, loss of *Flcn* expression in type II alveolar cells (lung progenitor cells) resulted in alveolar enlargement and epithelial cell apoptosis, suggesting that Flcn is required for the survival of normal lung progenitor cells (14). Recent evidence suggests that the kidney may also contain organ specific progenitor cell populations; therefore, it is tempting to speculate that the hyperproliferating cells detected in the kidney after conditional deletion of *Flcn* might include a previously uncharacterized kidney progenitor cell population, in addition to fully differentiated tubule and ductal epithelial cells (36, 37). Thus, Flcn may regulate progenitor cell homeostasis in the lung and kidney by maintaining quiescence, and its loss may contribute to cancer initiation in these and other organs by promoting the proliferation of a self-renewing progenitor population, which can acquire additional mutations with age. Additional studies will be needed to determine the requirement for Flcn in adult stem and progenitor cells from other organs, including the skin and gut, where the demand for differentiated cell populations is high.

Flcn is intrinsically required for HSPC survival, proliferation and differentiation, since mice transplanted with *Flcn* KO BMC showed impaired erythroid, B-cell and granulocyte lineage development. However, *Flcn* is expressed in many tissues (Fig S1B), therefore, it is likely that loss of *Flcn* may also affect cells in the hematopoietic microenvironment (4). We have observed that the bones of *Flcn* KO moribund mice are brittle, which suggests that Flcn might be required for proper niche function (unpublished observation). Therefore, future experiments are planned to determine if Flcn is required for proper microenvironment function, first, by transplanting *Flcn* WT BMC into *Flcn* KO irradiated recipient mice. Furthermore, it will be informative to conditionally inactivate *Flcn* in specific cell lineages within the Niche.

While loss of *Flcn* results in early embryonic lethality in conventional KO mice(4), mice that lack *Fnip1*, a critical binding partner of Flcn, develop normally, but show a developmental block in B cell development at the pro-B cell stage (38). Since Fnip1 and Fnip2 are

expressed in most tissues, and *Fnip2* KO mice show normal development, it is possible that Fnip2 may compensate for the loss of Fnip1 in HSPC (12, 39). In this regard, kidney tumors develop in mice when both *Fnip1* and *Fnip2* are conditionally inactivated, suggesting a functional redundancy in kidney function (39). Thus, we speculate that loss of Fnip1 and Fnip 2 in HSC would result in a dramatic loss of HSPC and bone marrow failure.

Although activation of mTorc1 signaling has been demonstrated in human and some mouse kidney cells upon loss of *Flcn* and contributes to renal cell hyperproliferation, mTorc1 activation is not always observed, and is thought to be dependent on the cell type and experimental conditions/contexts(7, 40). In fact, FLCN has been shown to be required for mTORC1 activation by amino acid stimulation in human embryonic kidney cells (40). Here, we demonstrate that mTorc1 is activated in BMC upon loss of *Flcn*, and confirm that this pathway is activated *in vivo*, since the splenomegaly observed after conditional inactivation of *Flcn* can be partially rescued by treating mice with rapamycin. In addition, we found that spleen progenitors from *Flcn* KO mice show enhanced proliferation *in vitro*, and that proliferation of these progenitor cells was inhibited by rapamycin in a dose dependent manner, suggesting that this pathway, in part, drives the splenic hyperplasia. Inactivation of *Pten* and *Tsc1* function in hematopoietic cells activates mTorc1 and leads to HSC proliferation and exhaustion, and in some cases leukemia, and these phenotypes can be partially rescued by rapamycin *in vivo* (21, 23, 28, 29, 41, 42). Finally, mice with loss of Ampk1/2 function do not show a hematopoietic phenotype, while mice with loss of Akt function undergo quiescence, suggesting that mTorc1 is mainly activated by Akt in *Flcn* KO BMC (24). Thus, the hematopoietic phenotypes in mice with aberrantly activated mTorc1 signaling are similar to those observed in our *Flcn* KO mouse model, and support the conclusion that activation of mTorc1 may represent one mechanism by which loss of *Flcn* contributes to hematopoietic failure.

Tfe3 is sequestered in the cytoplasm in Flcn-containing complexes in normal kidney cells and ES cells, and suppresses the transcriptional activity of Tfe3 by preventing its localization to the nucleus (32, 34). Here we report, that Tfe3 is localized most predominantly in the nucleus in *Flcn* KO HSC compared to control HSC and that Tfe3 overexpression in HSPC dramatically reduces the function of HSC in BMT assays, supporting the conclusion that localization of Tfe3 to the nucleus of *Flcn* KO HSC contributes to the reduced HSC activity. However, the precise molecular mechanism(s) by which Tfe3 regulates HSC development, and Tfe3 target genes remain to be investigated.

It was unexpected that *Flcn* inactivation would cause an acute histiocytosis and hemophagocytosis of hematopoietic cells. *Flcn* inactivation after BMT recapitulated the histiocytosis and hemophagocytosis demonstrating that these phenotypes were due to the cell intrinsic loss of *Flcn*. Interestingly, Tfe3 regulates macrophage differentiation (43); therefore, future studies will conditionally inactivate *Flcn* in the monocyte/macrophage lineage to determine if loss of Flcn affects macrophage development and activity, and promotes a histocytosis. These studies could potentially provide novel insights into the molecular mechanism(s) that regulate macrophage activity, and a potential mouse model of histiocytosis.

Summary

The results of gene inactivation studies in mouse kidney, lung and embryonic stem cells (ESCs) suggest that *Flcn* may regulate stem cell proliferation and differentiation, and may be required to maintain adult stem cell populations in these and other organs. In this study, we demonstrate that loss of *Flcn* expression in adult BMCs disrupts HSC quiescence and rapidly promotes HSPC hyperproliferation and stem cell exhaustion, and loss of all hematopoietic cell lineages leading to acute BM failure. The discovery that mTorc1 is activated in HSPC by loss of *Flcn* suggests a likely mechanism for loss of quiescence in adult stem cells. In addition the Flcn-Tfe3 pathway may also represent a new mechanism to regulate HSPC development.

Supplementary Material

Refer to Web version on PubMed Central for supplementary material.

Acknowledgments

We wish to thank Mr. Steven Stull, Ms.Terri Stull and Louise Cromwell for excellent animal technical support. This work was supported by the Intramural Research Program of the National Institutes of Health (NIH), National Cancer Institute (NCI), and Center for Cancer Research, and by Keio University Grant-in-Aid for Encouragement of Young Medical Scientists, by BioLegend / Tomy Digital Biology Research Grant Program 2013 (Latter Term). T.S. and M.B. were supported in part by a JSPS KAKENHI Grant-in-Aid for Scientific Research (S). M.B. was supported by JSPS KAKENHI, Grant-in-Aid for Scientific Research (B), Grant Number 15H04975; and Grant-in-Aid for Challenging Exploratory Research, Grant Number 15K14370. This project has been funded in part with Federal funds from the Frederick National Laboratory for Cancer Research, NIH, under Contract HHSN261200800001E. The content of this publication does not necessarily reflect the views or policies of the Department of Health and Human Services, nor does mention of trade names, commercial products or organizations imply endorsements by the US Government. NCI-Frederick is accredited by AAALAC International and follows the Public Health Service Policy for the Care and Use of Laboratory Animals. Animal care was provided in accordance with the procedures outlined in the “Guide for Care and Use of Laboratory Animals “(National Research Council; 1996; National Academy Press; Washington DC).

References

1. Nickerson ML, et al. Mutations in a novel gene lead to kidney tumors, lung wall defects, and benign tumors of the hair follicle in patients with the Birt-Hogg-Dube syndrome. Cancer cell. 2002; 2(2): 157–164. [PubMed: 12204536]
2. Birt AR, Hogg GR, Dube WJ. Hereditary multiple fibrofolliculomas with trichodiscomas and acrochordons. Archives of dermatology. 1977; 113(12):1674–1677. [PubMed: 596896]
3. Zbar B, et al. Risk of renal and colonic neoplasms and spontaneous pneumothorax in the Birt-Hogg-Dube syndrome. Cancer epidemiology, biomarkers & prevention : a publication of the American Association for Cancer Research, cosponsored by the American Society of Preventive Oncology. 2002; 11(4):393–400.
4. Hasumi Y, et al. Homozygous loss of BHD causes early embryonic lethality and kidney tumor development with activation of mTORC1 and mTORC2. Proc Natl Acad Sci U S A. 2009; 106(44): 18722–18727. [PubMed: 19850877]
5. Baba M, et al. Kidney-targeted Birt-Hogg-Dube gene inactivation in a mouse model: Erk1/2 and Akt-mTOR activation, cell hyperproliferation, and polycystic kidneys. Journal of the National Cancer Institute. 2008; 100(2):140–154. [PubMed: 18182616]
6. Chen J, et al. Deficiency of FLCN in mouse kidney led to development of polycystic kidneys and renal neoplasia. PLoS One. 2008; 3(10):e3581. [PubMed: 18974783]
7. Hudon V, et al. Renal tumour suppressor function of the Birt-Hogg-Dube syndrome gene product folliculin. J Med Genet. 2010; 47(3):182–189. [PubMed: 19843504]

8. Vocke CD, et al. High frequency of somatic frameshift BHD gene mutations in Birt-Hogg-Dube-associated renal tumors. Journal of the National Cancer Institute. 2005; 97(12):931–935. [PubMed: 15956655]
9. Schmidt LS. Birt-Hogg-Dube syndrome: from gene discovery to molecularly targeted therapies. Familial cancer. 2013; 12(3):357–364. [PubMed: 23108783]
10. Tee AR, Pause A. Birt-Hogg-Dube: tumour suppressor function and signalling dynamics central to folliculin. Familial cancer. 2013; 12(3):367–372. [PubMed: 23096221]
11. Baba M, et al. Folliculin encoded by the BHD gene interacts with a binding protein, FNIP1, and AMPK, and is involved in AMPK and mTOR signaling. Proc Natl Acad Sci U S A. 2006; 103(42): 15552–15557. [PubMed: 17028174]
12. Hasumi H, et al. Identification and characterization of a novel folliculin-interacting protein FNIP2. Gene. 2008; 415(1–2):60–67. [PubMed: 18403135]
13. Shaw RJ. LKB1 and AMP-activated protein kinase control of mTOR signalling and growth. Acta physiologica. 2009; 196(1):65–80. [PubMed: 19245654]
14. Goncharova EA, et al. Folliculin controls lung alveolar enlargement and epithelial cell survival through E-cadherin, LKB1, and AMPK. Cell reports. 2014; 7(2):412–423. [PubMed: 24726356]
15. Hasumi Y, et al. Folliculin (Flcn) inactivation leads to murine cardiac hypertrophy through mTORC1 deregulation. Human molecular genetics. 2014; 23(21):5706–5719. [PubMed: 24908670]
16. Anonymous.
17. Hartman TR, et al. The role of the Birt-Hogg-Dube protein in mTOR activation and renal tumorigenesis. Oncogene. 2009; 28(13):1594–1604. [PubMed: 19234517]
18. Hong SB, et al. Tumor suppressor FLCN inhibits tumorigenesis of a FLCN-null renal cancer cell line and regulates expression of key molecules in TGF-beta signaling. Molecular cancer. 2010; 9:160. [PubMed: 20573232]
19. Cash TP, Gruber JJ, Hartman TR, Henske EP, Simon MC. Loss of the Birt-Hogg-Dube tumor suppressor results in apoptotic resistance due to aberrant TGFbeta-mediated transcription. Oncogene. 2011; 30(22):2534–2546. [PubMed: 21258407]
20. Magee JA, Piskounova E, Morrison SJ. Cancer stem cells: impact, heterogeneity, and uncertainty. Cancer cell. 2012; 21(3):283–296. [PubMed: 22439924]
21. Yilmaz OH, et al. Pten dependence distinguishes haematopoietic stem cells from leukaemia-initiating cells. Nature. 2006; 441(7092):475–482. [PubMed: 16598206]
22. Soderberg SS, Karlsson G, Karlsson S. Complex and context dependent regulation of hematopoiesis by TGF-beta superfamily signaling. Annals of the New York Academy of Sciences. 2009; 1176:55–69. [PubMed: 19796233]
23. Zhang J, et al. PTEN maintains haematopoietic stem cells and acts in lineage choice and leukaemia prevention. Nature. 2006; 441(7092):518–522. [PubMed: 16633340]
24. Nakada D, Saunders TL, Morrison SJ. Lkb1 regulates cell cycle and energy metabolism in haematopoietic stem cells. Nature. 2010; 468(7324):653–658. [PubMed: 21124450]
25. Clements WK, Traver D. Signalling pathways that control vertebrate haematopoietic stem cell specification haematopoietic stem cell specification. Nature reviews. Immunology. 2013; 13(5): 336–348.
26. Orkin SH, Zon LI. Hematopoiesis: an evolving paradigm for stem cell biology. Cell. 2008; 132(4): 631–644. [PubMed: 18295580]
27. Trumpp A, Essers M, Wilson A. Awakening dormant haematopoietic stem cells. Nature reviews. Immunology. 2010; 10(3):201–209.
28. Gan B, et al. mTORC1-dependent and -independent regulation of stem cell renewal, differentiation, and mobilization. Proc Natl Acad Sci U S A. 2008; 105(49):19384–19389. [PubMed: 19052232]
29. Chen C, et al. TSC-mTOR maintains quiescence and function of hematopoietic stem cells by repressing mitochondrial biogenesis and reactive oxygen species. J Exp Med. 2008; 205(10):2397–2408. [PubMed: 18809716]

30. Kim W, Klarmann KD, Keller JR. Gfi-1 regulates the erythroid transcription factor network through Id2 repression in murine hematopoietic progenitor cells. Blood. 2014; 124(10):1586–1596. [PubMed: 25051963]
31. Kuhn R, Schwenk F, Aguet M, Rajewsky K. Inducible gene targeting in mice. Science. 1995; 269(5229):1427–1429. [PubMed: 7660125]
32. Hong SB, et al. Inactivation of the FLCN tumor suppressor gene induces TFE3 transcriptional activity by increasing its nuclear localization. PLoS One. 2010; 5(12):e15793. [PubMed: 21209915]
33. Petit CS, Roczniak-Ferguson A, Ferguson SM. Recruitment of folliculin to lysosomes supports the amino acid-dependent activation of Rag GTPases. The Journal of cell biology. 2013; 202(7):1107–1122. [PubMed: 24081491]
34. Betschinger J, et al. Exit from pluripotency is gated by intracellular redistribution of the bHLH transcription factor Tfe3. Cell. 2013; 153(2):335–347. [PubMed: 23582324]
35. Singh SR, et al. The Drosophila homolog of the human tumor suppressor gene BHD interacts with the JAK-STAT and Dpp signaling pathways in regulating male germline stem cell maintenance. Oncogene. 2006; 25(44):5933–5941. [PubMed: 16636660]
36. Kitamura S, Sakurai H, Makino H. Single Adult Kidney Stem/Progenitor Cells Reconstitute 3-Dimensional Nephron Structures in Vitro. Stem Cells. 2014
37. Wang HL, Liu NM, Li R. Role of adult resident renal progenitor cells in tubular repair after acute kidney injury. Journal of integrative medicine. 2014; 12(6):469–475. [PubMed: 25412664]
38. Baba M, et al. The folliculin-FNIP1 pathway deleted in human Birt-Hogg-Dube syndrome is required for murine B-cell development. Blood. 2012; 120(6):1254–1261. [PubMed: 22709692]
39. Hasumi H, et al. Folliculin-interacting proteins Fnip1 and Fnip2 play critical roles in kidney tumor suppression in cooperation with Flcn. Proc Natl Acad Sci U S A. 2015; 112(13):E1624–E1631. [PubMed: 25775561]
40. Tsun ZY, et al. The folliculin tumor suppressor is a GAP for the RagC/D GTPases that signal amino acid levels to mTORC1. Mol Cell. 2013; 52(4):495–505. [PubMed: 24095279]
41. Magee JA, et al. Temporal changes in PTEN and mTORC2 regulation of hematopoietic stem cell self-renewal and leukemia suppression. Cell Stem Cell. 2012; 11(3):415–428. [PubMed: 22958933]
42. Kalaitzidis D, et al. mTOR complex 1 plays critical roles in hematopoiesis and Pten-loss-evoked leukemogenesis. Cell Stem Cell. 2012; 11(3):429–439. [PubMed: 22958934]
43. Zanocco-Marani T, et al. Tfe3 expression is closely associated to macrophage terminal differentiation of human hematopoietic myeloid precursors. Experimental cell research. 2006; 312(20):4079–4089. [PubMed: 17046750]

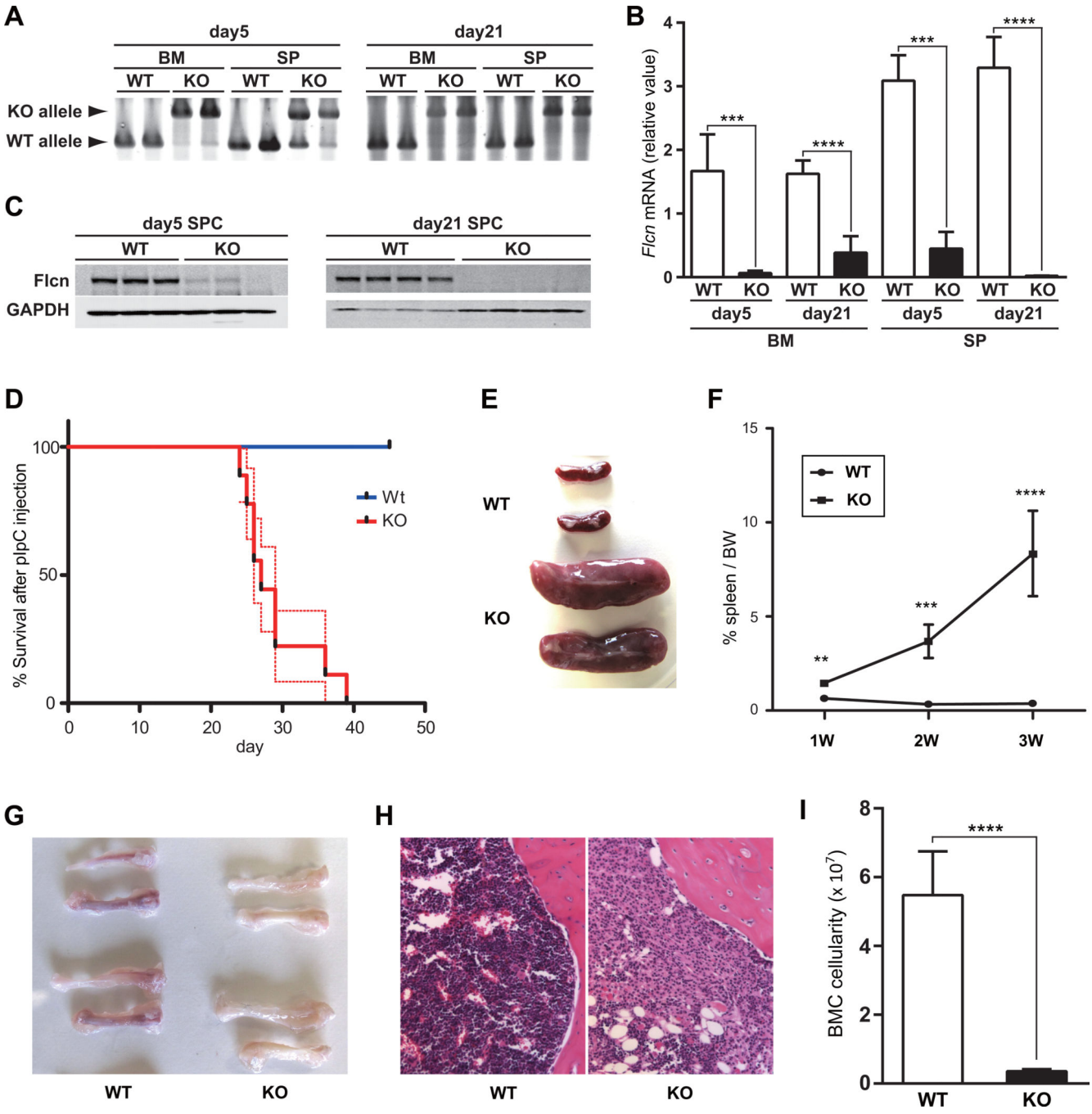

Figure 1. *Flcn* deletion in bone marrow disrupts normal hematopoiesis

(A) Bone marrow cells (BMC) and splenocytes (SPC) were isolated from *Flcn*$^{f/f}$;*Mx1-Cre*$^{-}$ (*Flcn* WT) and *Flcn*$^{f/f}$;*Mx1-Cre*$^{+}$ (*Flcn* KO) mice on day 5 and day 21 after pIpC treatment. PCR genotyping demonstrated efficient deletion of *Flcn* in bone marrow (BM) and spleen (SP). (B) *Flcn* mRNA expression in BM was quantified by quantitative reverse transcription-polymerase chain reaction (qRT-PCR) on day 5 and day 21 after pIpC treatment (Y-axis). BM day 5, BM day 21 and SP day 21: n=5 mice for each genotype; SP day 5:n=3 mice for each genotype. Data are presented as mean with SD (unpaired student's t-test: ****P<.0001,

P<.001). (C) Efficient suppression of Flcn protein expression was also confirmed by western blotting on day 5 and day 21 after pIpC treatment. (D) Kaplan-Meier survival analysis shows a statistically significant difference between control and *Flcn* KO (log-rank test: ****P<.0001). Median survival time of *Flcn* KO mice is 27 days after pIpC treatment (n=9). Dotted lines indicate SEM. (E) Gross images of spleens from *Flcn* WT and *Flcn* KO mice at day 28 after pIpC treatment show symmetrical enlargement of *Flcn* KO spleen compared with *Flcn* WT spleen. One representative image of more than 10 mice is shown. (F) % spleen/body weight (BW); spleen weight/BW × 100 was calculated at different day after pIpC treatment. The mean % spleen/body weights of *Flcn* WT and *Flcn* KO mice are 0.64±0.18% vs 1.47±0.22% (**P=.01) at day 7 (1W), 0.33±0.08% vs 3.68±0.89% (P=.0003) at day 14 (2W) and 0.37±0.09% vs 8.34±2.27% (****P<.0001) at day 21 (3W) determined using unpaired student's t-test. n=4 for each group on day 7 and 14, n=5 for each group on day 21. Data are represented as means ± SD. (G) Gross images of femurs and tibiae from *Flcn* WT and *Flcn* KO mice at day 21 after pIpC treatment show pale BM in *Flcn* KO mice. One representative image of more than 10 mice for each genotype is shown. (H) H & E staining of bone marrow from *Flcn* WT and *Flcn* KO mice at day 21 after pIpC treatment shows hypoplastic *Flcn* KO BM. One representative image of 3 mice for each genotype. (I) Absolute cell numbers of BMC from femurs and tibiae of *Flcn* WT and *Flcn* KO mice at day 21 ($5.48\pm1.27 \times 10^7$ vs $0.35\pm0.06 \times 10^7$, unpaired student's t-test: ****P<.0001). n=5 for each group. Data are represented as means± SD.

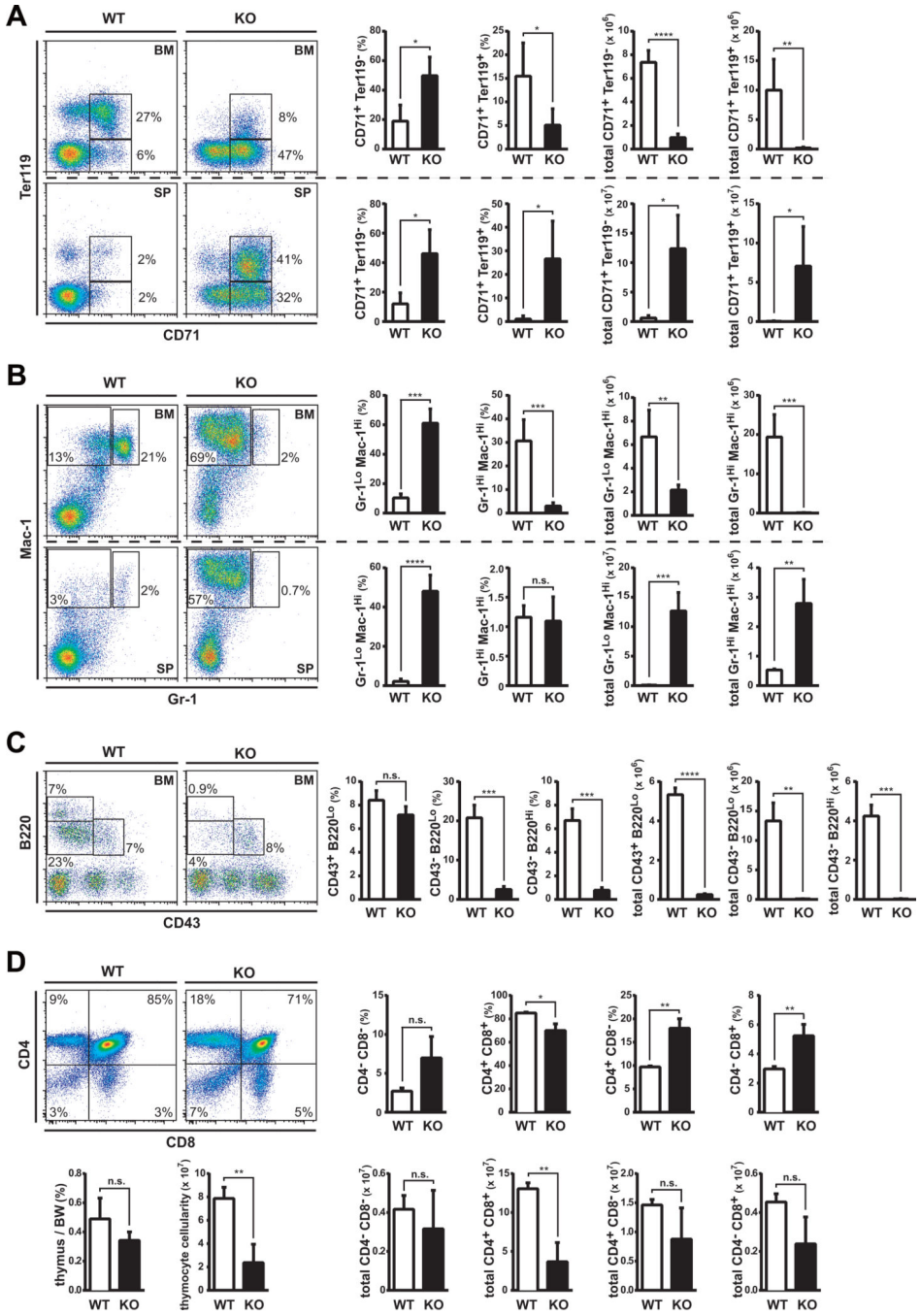

Figure 2. Flcn is required for the development of erythroid, myeloid and lymphoid cell lineages

(A-D) Flow cytometry analysis of BMC, SPC and thymocytes from *Flcn* WT and *Flcn* KO mice at day 21 after pIpC treatment. Graphs represent percentage (%) of the population and absolute number. (A) CD71 × Ter119 analysis of BMC reveals a defect in erythroid development, with an increase in pro-erythroblasts (*Flcn* WT vs *Flcn* KO $CD71^{+}Ter119^{-}$ BMC: 19.0% vs. 49.8%, $*P<0.05$), and loss of erythroblasts (*Flcn* WT vs *Flcn* KO: total $CD71^{+}Ter119^{+}$ BMC: 15.5% vs 5.1%, $*P<0.05$). BM data in upper panels and SP data in lower panels (*Flcn* WT, n=3; *Flcn* KO, n=5). (B) Mac-1 × Gr-1 analysis reveals a neutrophil

developmental defect and expansion of Mac-1^{+}Gr-1^{lo} and Mac-1^{+}Gr-1^{-} cells in *Flcn* KO mice. (*Flcn* WT, n=3; *Flcn* KO, n=5). (*Flcn* WT vs. *Flcn* KO Mac-1^{+}Gr-1^{hi}: 30.6% vs. 3.0%, ***P=0.0004 ; *Flcn* WT vs. *Flcn* KO Mac-1^{+}Gr-1^{lo} and Mac-1^{+}Gr-1^{-}: 10.3% vs. 61.1%, ***P=0.0001) (C) CD43 × B220 analysis shows B cell developmental arrest at progenitor-B cell stage in *Flcn* KO mice (*Flcn* WT, n=3; *Flcn* KO, n=3). (*Flcn* WT vs. *Flcn* KO CD43^{-}B220^{lo}: 20.8% vs. 2.5%, ***P=0.0007; *Flcn* WT vs. *Flcn* KO CD43^{-}B220^{hi}: 6.7% vs. 0.8%, ***P=0.0005). (D) CD8 × CD4 analysis of thymocytes shows reduced CD4^{+}CD8^{+} cell population in *Flcn* KO mice (*Flcn* WT, n=3; *Flcn* KO, n=3). (*Flcn* WT vs. *Flcn* KO CD4^{+}CD8^{+}: 13.04×10^{7} vs. 3.68×10^{7}, p<0.01). Data are represented as means±SD. (n.s. not significant, unpaired student's t-test: *P <.05, **P <.01, ***P <.001, ****P <.0001)

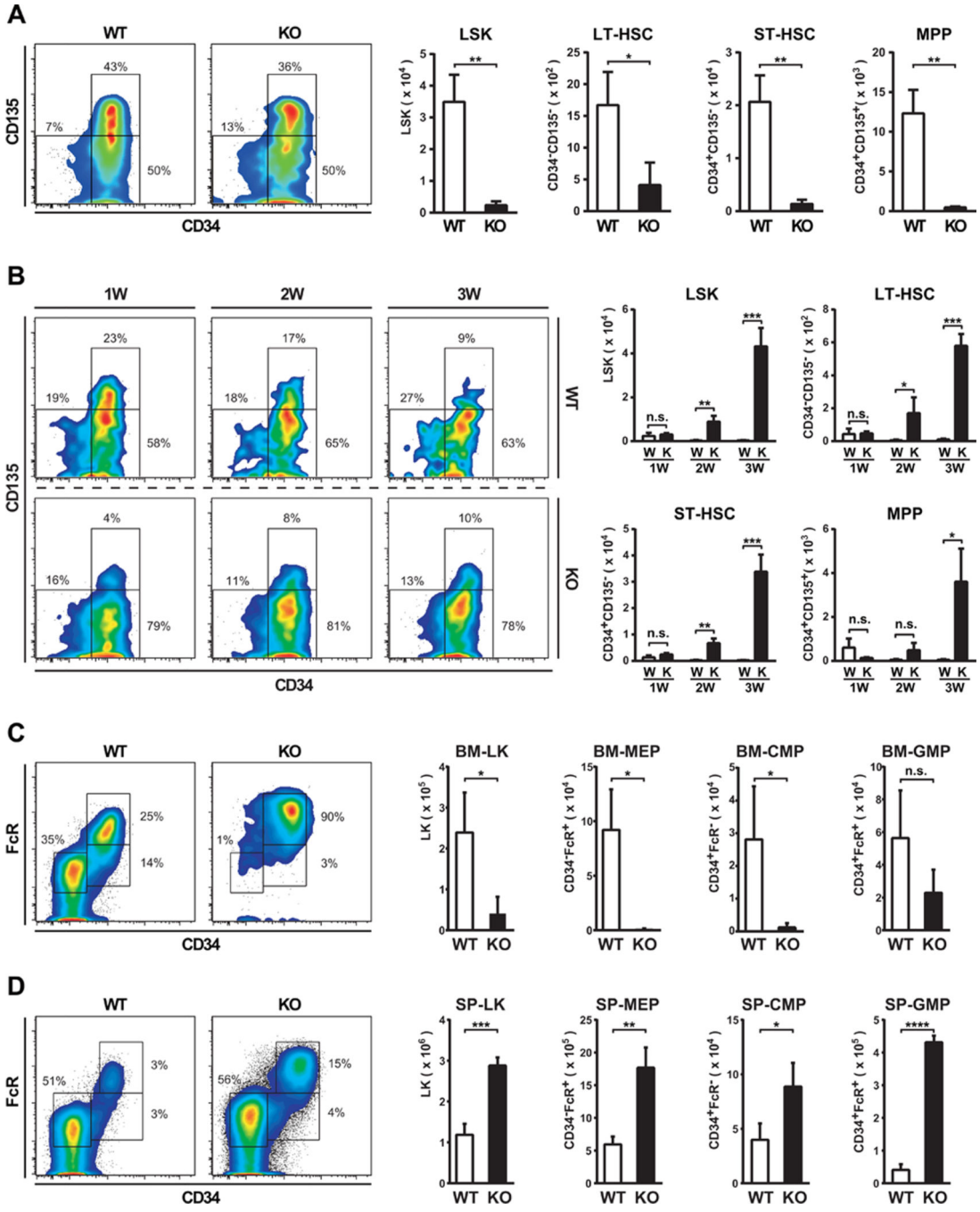

Figure 3. HSPC exhaustion and bone marrow failure in *Flcn* KO mice

(A) Flow cytometric analysis of HSPC in BM on day 7. The absolute number of Lin^{-}Sca1^{+}c-Kit^{+} (LSK) cells in *Flcn* KO BM was significantly reduced compared to *Flcn* WT BM. (*Flcn* WT vs *Flcn* KO: 34929±8570 vs 2342±1266, $^{**}P<.01$). n=3 for each group. The absolute number of LT-HSC (LSK CD34^{-}CD135^{-}), ST-HSC (LSK CD34^{+}CD135^{-}), and multipotent progenitors (MPP) (LSK CD34^{+}CD135^{+}) in *Flcn* KO BM were significantly reduced compared to *Flcn* WT BM. (*Flcn* WT vs *Flcn* KO LT-HSC: 1670±522 vs 408±357, $^{*}P<.05$), (*Flcn* WT vs *Flcn* KO ST-HSC: 20674±5015 vs 1373±752, $^{**}P<$.

01), (*Flcn* WT vs *Flcn* KO MPP: 12327±2973 vs 456±137, ***P* <.01), n=3 for each group. (B) Flow cytometry analysis of HSPC in SP on day 7, 14, and 21. Immunophenotypically defined HSPCs (LSK, LT-HSC, ST-HSC, MPP) increased in *Flcn* KO spleen significantly beginning day 14. n=3 for each group. (C) Flow cytometric analysis of progenitors in BM. $Lin^{-}Sca1^{-}c\text{-}Kit^{+}$ (LK) cells were significantly reduced in *Flcn* KO BM. MEP ($CD34^{-}FcR^{-}$), and CMP ($CD34^{+}FcR^{-}$) were also significantly reduced in *Flcn* KO BM. Although GMP ($CD34^{+}FcR^{+}$) showed a trend toward reduced numbers in *Flcn* KO BM, it was not statistically significant. n=3 for each group. (D) Flow cytometry analysis of progenitors in SP. All the immunophenotypically defined progenitor populations, LK, MEP, CMP, and GMP were statistically significantly increased in *Flcn* KO spleen. (A-D) (n.s. not significant, unpaired student's t-test: **P* <.05, ***P* <.01, ****P* <.001, *****P* <.0001) n=3 for each group.

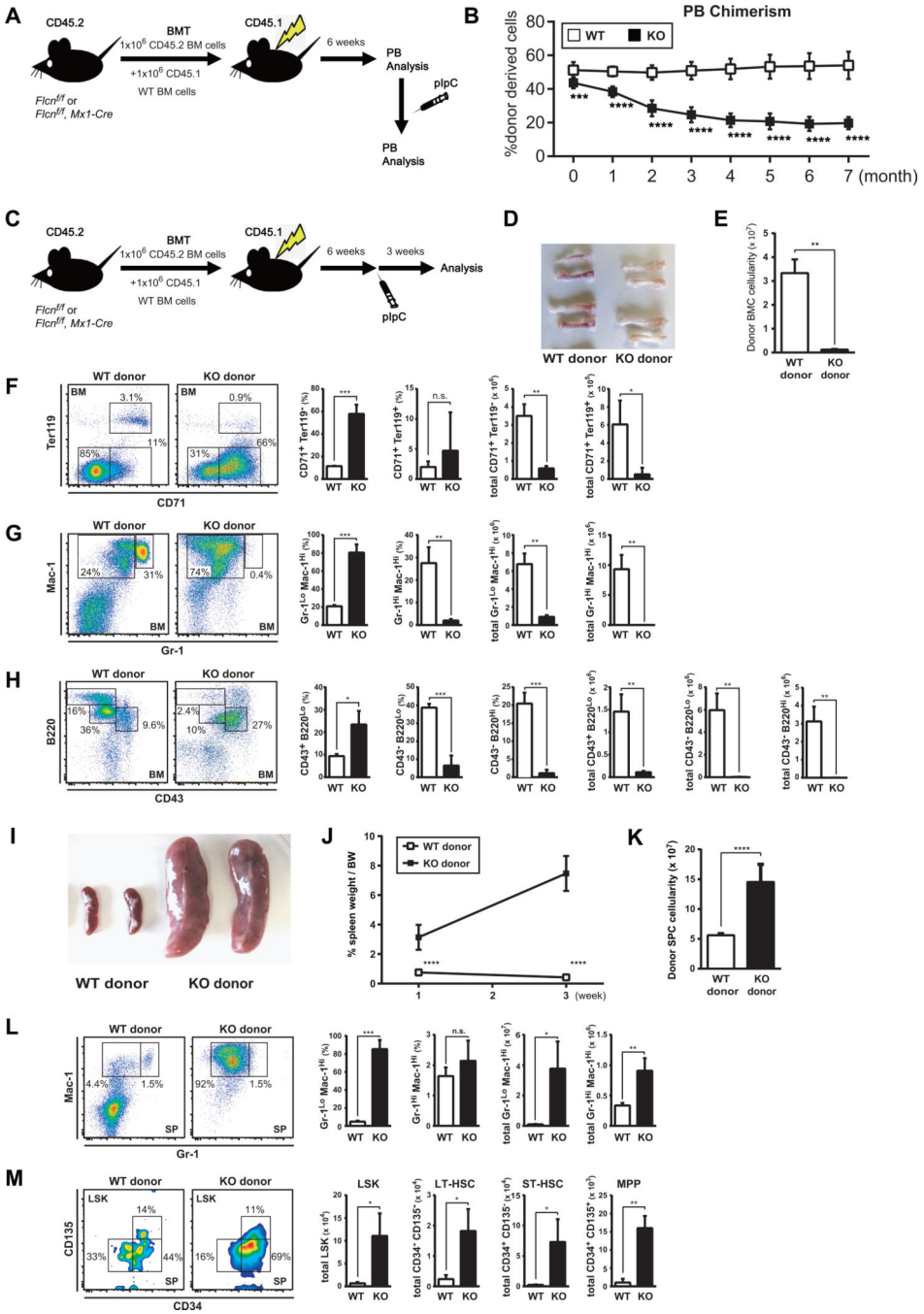

Figure 4. *Flcn* functions in a cell-autonomous manner during HSPC development

(A) Scheme of competitive BM transplantation (BMT) assay. 1×10^6 BM cells from CD45.2 control *Flcn* WT or *Flcn* KO mice were transplanted with 1×10^6 BM cells from CD45.1 C57BL/6J mice into lethally irradiated recipient CD45.1 C57BL/6J mice. Six weeks after BMT, pIpC was injected. (B) PBC chimerism measured by flow cytometry at different time points indicates the defective long-term reconstitution (LTR) activity of *Flcn* KO HSPCs. Data are presented as means ± SD (n=8, unpaired student's t-test: ***$P<.001$, ****$P<.0001$). (C) Scheme of BM transplantation (BMT) assay. 1×10^6 BM cells from CD45.2

control *Flcn* WT or *Flcn* KO mice were transplanted into lethally irradiated recipient CD45.1 C57BL/6J mice. Six weeks after BMT, pIpC was injected. Three weeks after pIpC injection, BM cells and splenocytes were analyzed by flow cytometry. (D) Gross images of femurs and tibiae of recipient mice transplanted with CD45.2 WT or KO BM cells at day 21 show pale BM in *Flcn* KO BM cells transplanted donors. One representative image of more than 10 mice for each group is shown. (E) Absolute donor derived CD45.2 cell numbers of BMC from femurs and tibiae of recipient mice at day 21 ($3.33\pm0.57 \times 10^7$ vs $0.12\pm0.03 \times 10^7$, unpaired student's t-test: $^{**}P<.01$). n=3 for each group. Data are represented as means ± SD. (F-H) Flow cytometry analysis of BMC from recipient mice transplanted with *Flcn* WT and *Flcn* KO BMC. Results recapitulated the defective hematopoiesis phenotype of the original *Flcn* KO mice. Each analysis is representative of at least three independent experiments. Graphs represent percentage (%) of the population and absolute number. (F) CD71 × Ter119 analysis reveals a defect in erythroid development, with an increase in pro-erythroblasts (*Flcn* WT vs *Flcn* KO $CD71^+Ter119^-$: 11.4% vs. 57.8%, unpaired student's t-test: $^{***}P=0.0006$). (n=3 for each group). (G) Mac-1 × Gr-1 analysis reveals a neutrophil developmental defect and expansion of Mac-1^+Gr-1^{lo} and Mac-1^+Gr-1^- cells in *Flcn* KO BMC transplanted recipient mice. (n=3 for each group). (*Flcn* WT vs. *Flcn* KO Mac-1^+Gr-1^{hi}: 27.5% vs. 2.0%, unpaired student's t-test: $^{**}P=0.003$; *Flcn* WT vs. *Flcn* KO Mac-1^+Gr-1^{lo} and Mac-1^+Gr-1^-: 20.8% vs. 80.5%, unpaired student's t-test:$^{***}P=0.0003$) (H) CD43 × B220 analysis shows B cell developmental arrest at progenitor-B cell stage in *Flcn* KO BMC transplanted recipient mice. (n=3 for each group). (*Flcn* WT vs. *Flcn* KO $CD43^-B220^{lo}$: 38.7% vs. 6.5%, unpaired student's t-test: $^{***}P=0.0007$; *Flcn* WT vs. *Flcn* KO $CD43^-B220^{hi}$: 20.4% vs. 1.1%, unpaired student's t-test: $^{***}P=0.0005$). (I) Gross images of spleens from recipient mice transplanted with *Flcn* WT and *Flcn* KO BMC on day 21 after pIpC treatment show splenomegaly in *Flcn* KO BMC transplanted recipient mice. One representative image of more than 5 mice is shown. (J) % spleen/body weight (BW); spleen weight/BW × 100 was calculated at different days after pIpC treatment. The mean % spleen/body weights of *Flcn* WT BMC and *Flcn* KO BMC recipient mice are 0.76±0.13% vs 3.14±0.84% (unpaired student's t-test: $^{****}P<.0001$) at day 7 (1W) and 0.42±0.04% vs 7.47±1.18% (unpaired student's t-test: $^{***}P=0.0005$) at day 21 (3W). n=6 for each group on day 7, n=3 for each group on day 21. Data are represented as means ± SD. (K) Absolute cell numbers of splenocytes from recipient mice transplanted with *Flcn* WT and *Flcn* KO donor BMC at day 21 after pIpC treatment ($5.60\pm0.37 \times 10^7$ vs $14.5\pm2.97 \times 10^7$, unpaired student's t-test: $^{**}P=0.007$). n=3 for each group. Data are represented as means± SD. (L) Flow cytometry analysis of splenocytes from recipient mice transplanted with *Flcn* WT and *Flcn* KO donor BMC at day 21 after pIpC treatment. Graphs represent percentage (%) of the population and absolute number. Mac-1 × Gr-1 analysis reveals an expansion of Mac-1^+Gr-1^{lo} and Mac-1^+Gr-1^- cells in recipient mice transplanted with *Flcn* KO donor BMC. ($0.10\pm0.0.3 \times 10^7$ vs $4.08\pm1.50 \times 10^7$, unpaired student's t-test:$^{*}P=0.01$). n=3 for each group. Data are represented as means± SD. (M) Flow cytometric analysis of splenocytes from recipient mice transplanted with *Flcn* WT and *Flcn* KO donor BMC at day 21 after pIpC treatment. The absolute number of $Lin^-Sca1^+c\text{-}Kit^+$ (LSK) cells, LT-HSC (LSK $CD34^-CD135^-$), ST-HSC (LSK $CD34^+CD135^-$), and multipotent progenitors (MPP) (LSK $CD34^+CD135^+$) in recipient mice transplanted with *Flcn* KO donor BMC were significantly increased compared to recipient mice transplanted with *Flcn* WT donor BMC.

(*Flcn* WT vs *Flcn* KO LSK: 0.67±0.27 × 10^4 vs 11.06±45.00 × 10^4, **P* <.05), (*Flcn* WT vs *Flcn* KO LT-HSC: 0.24±0.13 × 10^4 vs 1.82±0.72 × 10^4, **P* <.05), (*Flcn* WT vs *Flcn* KO ST-HSC: 0.24±0.07 vs 7.30±3.75, **P* <.05), (*Flcn* WT vs *Flcn* KO MPP: 1.05±1.02 vs 15.99±3.35, ***P* <.01), n=3 for each group. Data are represented as means± SD.

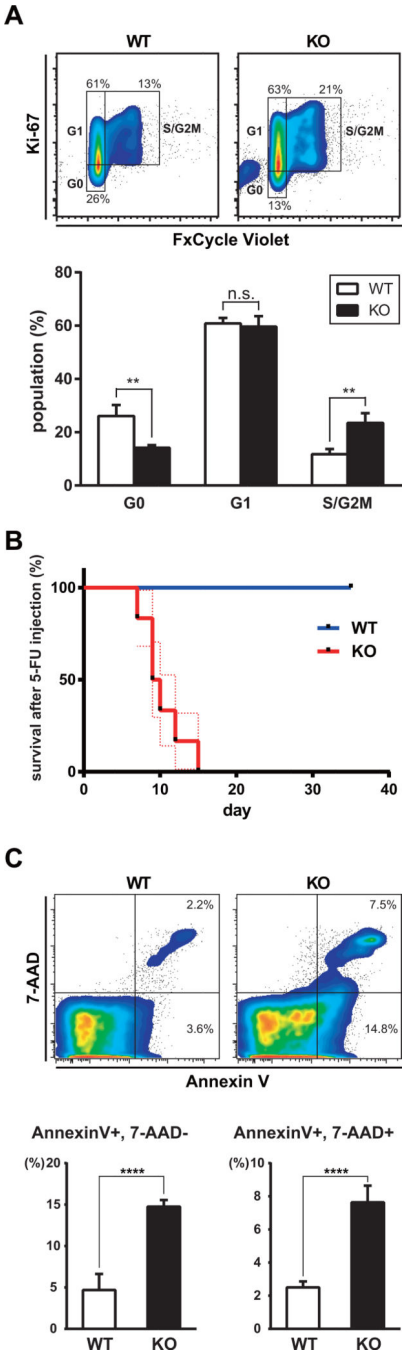

Figure 5. Essential role of Flcn in HSC quiescence and survival

(A) *Flcn* WT and *Flcn* KO mice were injected with pIpC. Five days after pIpC injection, BMC were isolated and stained with Lineage marker (CD4, CD8, B220, TER-119, Mac-1, and Gr-1), Sca-1, c-Kit, Ki67 and FxCycle Violet, followed by FACS analysis. *Flcn* KO LSK cells show significantly less Ki67^{-} G0 cells and more Ki-67^{+}, FxCycle Violet^{hi} S/G2M cells. (*Flcn* WT vs *Flcn* KO Ki67^{-}: 26.1±4.1% vs. 14.2±1.0%, unpaired student's t-test:**P=0.008; *Flcn* WT vs. *Flcn* KO Ki-67^{+}, FxCycle Violet^{hi}: 11.8±1.9% vs. 23.5±3.7%, unpaired student's t-test: **P=0.008). n=3 for each group. Data are represented as means±

SD. (B) To determine if HSPCs were actively dividing, a sublethal dose of 5-FU (100 mg/kg) was injected weekly starting one week after pIpC injection (day0). Kaplan-Meier survival analysis shows a statistically significant difference between *Flcn* WT and *Flcn* KO mice (log-rank test: ****P<.0001). Median survival time of *Flcn* KO mice was 9.5 days (n=6). Dotted lines indicate SEM. (C) Five days after pIpC injection, apoptotic cells in BMC were analyzed by Annexin V × 7-AAD staining using the Annexin V: PE Apoptosis Detection Kit (BD Biosciences). Annexin V^+, 7-AAD^- Early Apoptotic cells were significantly increased in *Flcn* KO BM (*Flcn* WT vs *Flcn* KO: 4.70±1.92 vs 14.77±0.79, unpaired student's t-test: ****P <.0001, n=6 for each group). Annexin V^+, 7-AAD^+ Late Apoptotic cells were also significantly increased in *Flcn* KO BM (*Flcn* WT vs *Flcn* KO: 2.50±0.36 vs 7.64±1.01, unpaired student's t-test: ****P <.0001, n=6 for each group). Data are represented as means ± SD.

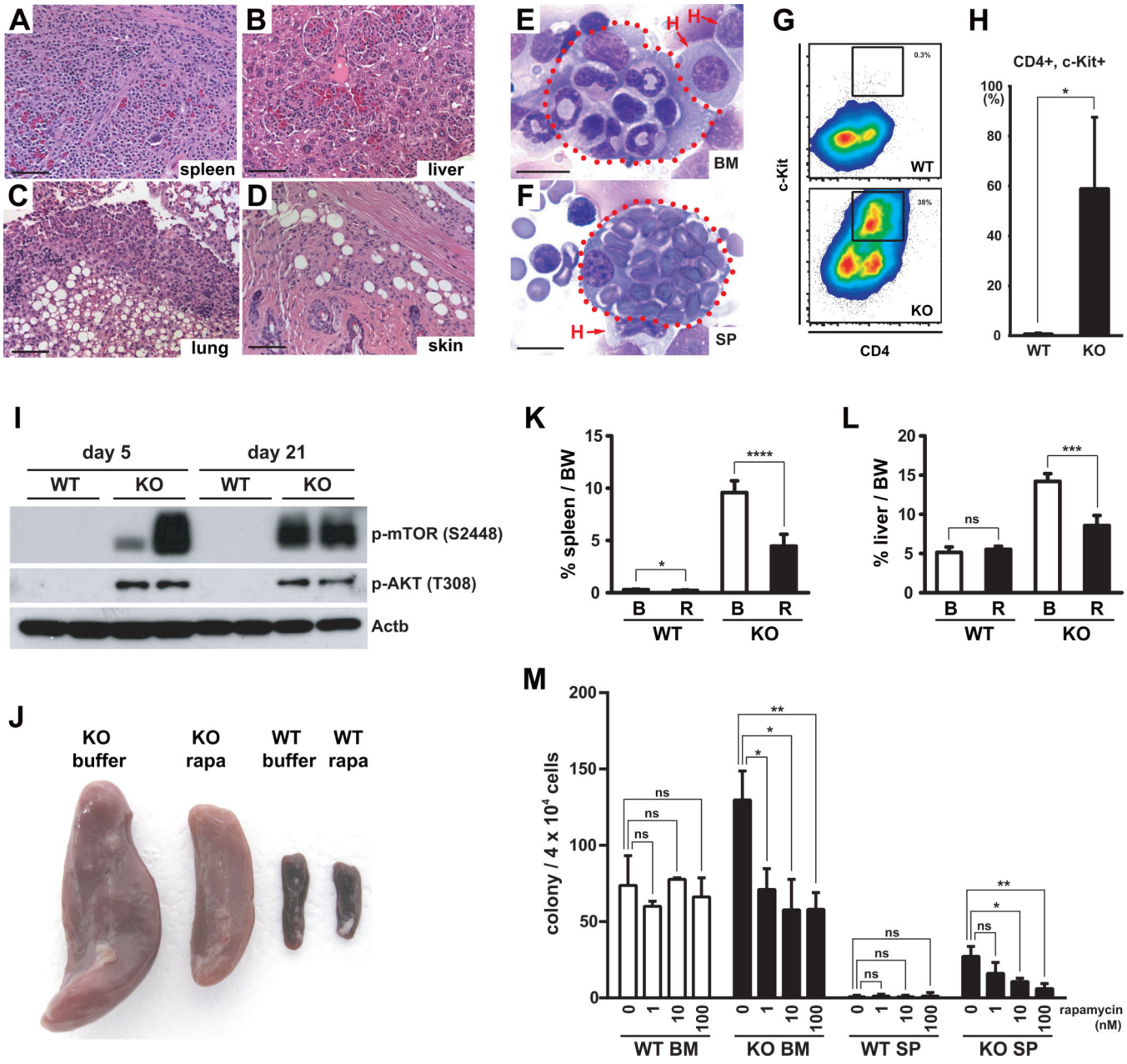

Figure 6. Histiocytosis in *Flcn* KO mice

(A-D) Histological analysis of *Flcn* KO: mouse tissues by H&E staining revealed systemic infiltration of histiocytes / macrophages in spleen (A), liver (B), lung (C), and skin (D). Scale bar=100μm. (E, F) Giemsa staining of cytocentrifuged BMC (E) and SP (F) in *Flcn* KO mice 14 days after pIpC injection shows histiocytes engulfing erythrocytes, neutrophils and lymphocytes. Scale bar=10μm. (G) Five days after pIpC treatment, Mac-1^{+}Gr-1^{lo} cells in *Flcn* KO BM show aberrant expression of CD4 and c-Kit. Representative of three independent experiments. (H) Significant increase of abnormal histiocytes expressing aberrant CD4 and c-Kit. (*Flcn* WT vs. *Flcn* KO :0.83±1.92% vs 59.03±28.57%, unpaired student's t-test: **P* < .05, n=3 for each group). Data are represented as means with SD. (I)

Five days after pIpC treatment, BMCs were isolated from *Flcn* WT and *Flcn* KO mice. BMC lysates were subjected to SDS-PAGE followed by western blotting. Representative data of three independent experiments. (J, K, L) Two mg/kg of rapamycin or buffer only were injected I.P. daily into *Flcn* WT and *Flcn* KO mice (n=7 for each group) starting on the last day of pIpC treatment for 24 days. At day 24, mice were dissected and body weight (BW), spleens and livers were weighed. (J) Gross images of spleens from buffer or rapamaycin treated *Flcn* WT and *Flcn* KO mice at day 24. Representative image of spleens from each group is shown. (K) The percent spleen weight/BW is shown. Rapamycin treatment of *Flcn* KO mice significantly reduced the percent spleen/body weight (buffer vs rapamycin: 9.59±1.12% vs 4.46±1.13%, unpaired student's t-test: ****P <.0001; n=7 for each group), while rapamycin had much less effect on *Flcn* WT mice (buffer vs rapamycin: 0.30±0.04% vs 0.24±0.04%, unpaired student's t-test: *P <.05; n=7 for each group). Data are represented as means ± SD. (L) The percent liver/BW is shown. Rapamycin treatment of *Flcn* KO mice significantly reduced the percent liver/body weight (buffer vs rapamycin: 14.22±0.98% vs 8.57±1.29%, unpaired student's t-test: ****P <.0001; n=7 for each group), while rapamycin had no effect on *Flcn* WT mice (*Flcn* WT vs *Flcn* KO: 5.14±0.71% vs 5.52±0.40%, unpaired student's t-test: n.s.- not significant, P=0.32; n=7 for each group). Data are represented as means ± SD. (M) The colony-forming units in culture (CFU-c) were measured to enumerate myeloid progenitor cells in BM and SP of *Flcn* WT and *Flcn* KO mice. BMC and SPC were isolated from pIpC-injected *Flcn* WT and *Flcn* KO mice on day 5, and 4×10^4 cells were plated on 3.5cm plates with different concentrations of rapamycin, and colony numbers were counted on day 10–14. Rapamycin significantly reduced the CFU-c of *Flcn* KO BM and spleen, while there was no effect on *Flcn* WT BM or spleen (n.s. not significant, unpaired student's t-test:*P <.05, **P <.01). Data are represented as means with SD. Representative data of two independent experiments.

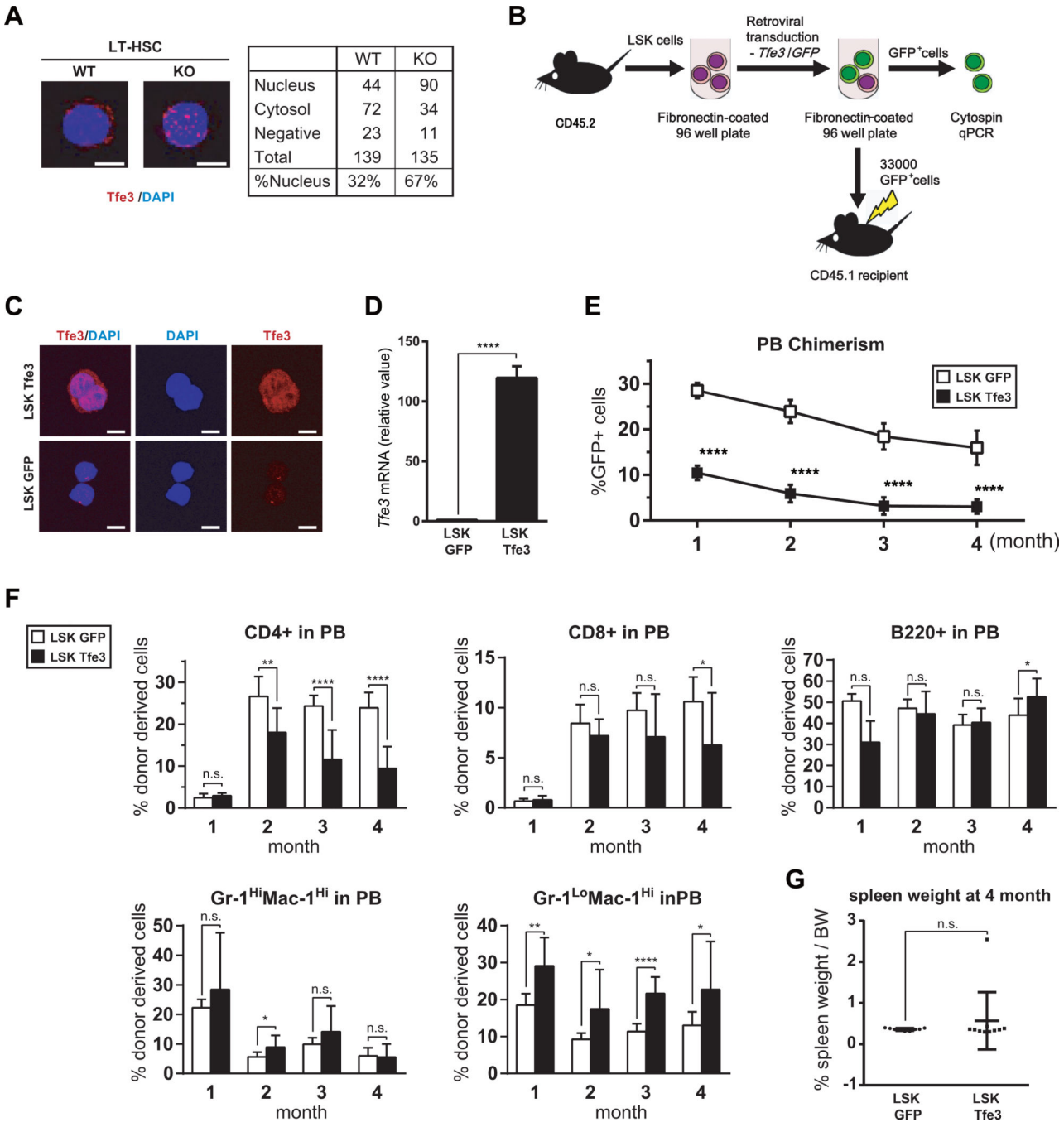

Figure 7. Aberrant activation of Tfe3 in *Flcn* KO HSPC and Tfe3 impairs long term reconstituting activity of HSPC

(A)Immunocytochemistry (ICC) of endogenous Tfe3 in LT-HSCs (LSK CD34^{-}CD135^{-}) from *Flcn* WT and *Flcn* KO mice. Tfe3 subcellular localization in LT-HSC was analyzed by counting Tfe3-expressing cells in the nucleus, cytosol or neither location. Photomicrographs are representative images of nuclear and cytosolic localization of Tfe3 in WT and KO LT-HSCs. More nuclear localization of Tfe3 was seen in *Flcn* KO LT-HSC compared to *Flcn* WT LT-HSC. (*Flcn* WT vs. *Flcn* KO : 32% vs 67%). (B) Scheme of the Tfe3 overexpression experiment in LSK cells. Approximately 50,000 *Flcn* WT LSK cells per well were cultured

on fibronectin-coated 96 well plates, and retrovirally transduced with *Tfe3* or *GFP* vector, respectively, using the CombiMag system. After retroviral transduction, 33,000 GFP positive cells (LSK GFP or LSK *Tfe3*) were transplanted into lethally irradiated CD45.1 *Flcn* WT mice. (C) ICC of Tfe3 in LSK cells transduced with *Tfe3* expression vector (LSK Tfe3) or *GFP* vector (LSK GFP) confirms Tfe3 overexpression by retrovirus transduction. (D) *Tfe3* overexpression in *Tfe3* transduced LSK cells was also confirmed by qRT-PCR on sorted GFP+ LSK cells. (E) PBC chimerism measured by flow cytometry at different time points after BMT demonstrates defective LTR activity of LSK Tfe3 cells unpaired student's t-test:**** $P < .0001$; LSK GFP, n=9; LSK Tfe3, n=10). Data are represented as means ± SD. Representative data of two independent experiments. (F) The percentages of each lineage among the GFP+ donor derived cells in peripheral blood were measured by FACS analysis. CD4+ T cells were significantly reduced among the LSK Tfe3 expressing donor derived cells. On the other hand, the population of Gr-1^{Lo}Mac-1^{Hi} cells was significantly increased (n.s. not significant, unpaired student's t-test: * $P < .05$, ** $P < .01$, **** $P < .0001$; LSK GFP, n=9; LSK Tfe3, n=10). Data are represented as means ± SD. Representative data of two independent experiments. (G) % spleen/body weight (BW) was calculated at 4 months after LSK cell transplantation. There was no statistically significant difference between LSK GFP transplanted mice and LSK Tfe3 transplanted mice. (LSK GFP vs LSK Tfe3: 0.36±0.03% vs 0.57±0.70%, unpaired student's t-test: n.s.- not significant ; LSK GFP, n=9; LSK Tfe3, n=10). Data are represented as means ± SD.